Ultrasonographic Characterization of Lingual Structures Pertinent to Oral, Periodontal and Implant Surgery

Shayan Barootchi[1], DMD, Hsun-Liang Chan[1], DDS, MS, Sharon S. Namazi[2] , DDS, Hom-Lay Wang[1] DDS, MS, PhD, and Oliver D Kripfgans[3,4], PhD

[1] Department of Periodontics & Oral Medicine, University of Michigan School of Dentistry, Ann Arbor, MI, USA

[2] Division of Anatomy, Department of Surgery, University of Michigan Medical School, Ann Arbor, MI

[3] Department of Biomedical Engineering, College of Engineering, Ann Arbor, Michigan

[4] Department of Radiology, University of Michigan Medical School, Ann Arbor, Michigan

Corresponding author:

Hsun-Liang Chan, Department of Periodontics and Oral Medicine, University of Michigan School of Dentistry, Ann Arbor, MI.

Email: hlchan@umich.edu

Phone: 734-272-1057

Word count: 3064

Figures and Tables: 1 table, 5 figures

Running title: Ultrasonographic Characterization of Lingual Structures

Keywords: ultrasonography, anatomy, alveolar ridge, diagnosis, dental implant

Abstract

Objectives: Increased applications of ridge augmentation in the lingual posterior mandible call for an urgent need to study its anatomy. Therefore, our first aim was to validate ultrasound in measuring the mandibular lingual structures in human cadavers. Secondarily, to test its feasibility in imaging the lingual nerve in live humans.

Materials and Methods: Nine fresh un-embalmed fully/partially edentulous cadaver heads were utilized for Aim 1. Three areas in the lingual mandible were imaged (mandibular premolar, molar, retromolar). Immediately after, biopsies were harvested from each site. The thickness of the mucosa, mylohyoid muscle, and lingual nerve diameter were measured via ultrasound and statistically compared to histology. Similarly, the lingual nerve in live humans was also imaged.

Results: None of the differences between the ultrasound and histology measurements reached statistical significance (*p>0.05*). The mean mucosal thickness via ultrasound and histology was 1.45±0.49, and 1.39±0.50 mm, 5 mm lingual to the mylohyoid muscle attachment. At 10 mm beyond the attachment, the ultrasound and histological values were 1.54±0.48, and 1.37±0.49, respectively. The mean muscle thickness measured via ultrasound and histology was 2.31±0.56, and 2.25±0.47 mm, at the 5 mm distance. At the 10 mm distance, the measurements were 2.46±0.56, and 2.36±0.5 mm, respectively. The mean ultrasonic lingual nerve diameter was 2.38±0.44 mm, versus 2.43±0.42 mm, with histology. The lingual nerve diameter on 19 live humans averaged to 2.01±0.35 mm (1.4 – 3.1 mm).

Conclusions: Within its limitations, ultrasound accurately measured mandibular lingual soft tissue structures on cadavers, and the lingual nerve on live humans.

1. Introduction

Clinicians are constantly faced with management of complex surgical cases requiring advanced and extensive tissue management. Successful management of these clinical scenarios for periodontal, oral surgery, or implant indications relies on a profound knowledge of the anatomical structures (Greenstein, Cavallaro, Romanos, & Tarnow, 2008; Tavelli, Barootchi, Namazi, et al., 2019; Tavelli, Barootchi, Ravida, Oh, & Wang, 2019). In particular, due to an increasing demand for augmenting atrophic posterior mandible and subsequent implant rehabilitation (Urban et al., 2017), a firm understanding of the biological structures in this region cannot be overemphasized. Surgical complications in the lingual posterior mandible may include mucosal tissue laceration, intrusion in

the sublingual space, trauma to the branches of the lingual artery, and injury to the lingual nerve, etc (Annibali, Ripari, La Monaca, Tonoli, & Cristalli, 2009; Camargo & Van Sickels, 2015; Greenstein et al., 2008; Isaacson, 2004; Longoni et al., 2007; Urban et al., 2017). These unfortunate adverse events may result in unfavorable bone augmentation outcomes, massive hemorrhage (Askar et al., 2019; Camargo & Van Sickels, 2015), neurosensory disturbances, and impaired mastication function. Therefore, successful flap release, and meticulous tissue management for achieving primary wound closure depends on a thorough anatomical understanding (Chan et al., 2010; Ritter et al., 2012; I. Urban et al., 2018; I. A. Urban et al., 2017).

In addition, it is now known that the quality and quantity of soft tissues greatly influence the healing of periodontal and implant procedures (Chao, Chang, Fu, Wang, & Chan, 2015; De Bruyckere, Eghbali, Younes, De Bruyn, & Cosyn, 2015; Fu et al., 2010; Lin, Chan, & Wang, 2013). This determines the tissue phenotype, which is currently evaluated through visual examination and probing (De Rouck, Eghbali, Collys, De Bruyn, & Cosyn, 2009; Eghbali, De Rouck, De Bruyn, & Cosyn, 2009). For instance, in the management of an extraction socket, tissue phenotype has been correlated with the amount of horizontal and vertical bone resorption that occurs following immediate implant placement (Ferrus et al., 2010). Other studies have shown its phenotypic feature in correlation with peri-implant marginal bone remodeling as well (Linkevicius, Apse, Grybauskas, & Puisys, 2009a, 2009b; Suarez-Lopez Del Amo, Lin, Monje, Galindo-Moreno, & Wang, 2016). Soft tissue features are a determinant of success of ridge augmentation and should be carefully evaluated before the surgery (Chen et al., 2017).

In medicine, the use of non-ionizing ultrasound has been established and advocated for many years (Bhaskar, Chan, MacEachern, & Kripfgans, 2018; Hoskins & Kenwright, 2015; Moskalik et al., 1995; Oelze & Mamou, 2016). In dentistry, its advantage for providing low-cost real-time cross-sectional images can be quite useful as it relates to providing optimal soft tissue contrast of pertinent anatomical structures and the peri-implant tissues (Bhaskar et al., 2018;

Chan, Sinjab, et al., 2017; Chan et al., 2018). Additionally, ultrasound has been validated for measuring tissue thickness in different locations of the oral cavity (Chan, Sinjab, et al., 2017; Chan, Wang, Fowlkes, Giannobile, & Kripfgans, 2017). A recent study from our group, applied and validated the use of ultrasound for accurate assessment of peri-implant tissues on human cadavers in comparison with direct visual and cone-beam computed tomography (CBCT) (Chan et al., 2018). In light of an increasing importance of the lingual anatomy, for the first time we applied our ultrasound probe prototype to characterize the lingual structures, i.e. the dimensions of the mucosa, mylohyoid muscle and lingual nerve, in comparison to histology. Feasibility of ultrasound to image the lingual nerve on live human patients was also investigated.

Materials and Methods

This project was prepared in accordance with the EQUATOR guidelines Standards for Reporting Qualitative Research (SRQR) (O'Brien, Harris, Beckman, Reed, & Cook, 2014).

2.1. Study Design of the cadaver research

Nine fresh un-embalmed fully/partially edentulous human cadaver heads were provided by the Department of Anatomy, to the Department of Periodontics and Oral Medicine of the University of Michigan. To reduce the occurrence of any structural tissue damages, all specimens were kept frozen at a controlled temperature of -20 degrees centigrade (without formalin fixation) after harvesting from the human donors. Immediately prior to utilization for the experiments, the specimens were thawed to room temperature. For inclusion in the present research, it was required that specimens were either completely edentulous or partially edentulous particularly in the mandibular arch (past the mandibular canine). No other eligibility criteria were imposed in regard to the cadavers. This study was exempted by the University of Michigan Institutional Review Board (IRB) under the application number HUM00168533.

2.2. Ultrasound Imaging and measures

The ultrasound equipment setups and the scanning procedures were performed by two experienced investigators (HC, OK) (Chan, Sinjab, et al., 2017; Chan, Wang, et al., 2017). Three distinct sites, the premolar, molar and retromolar sites, were selected for imaging (Figure 1). The initial scan was performed at the premolar site, identified in relation to the mental foramen, followed by the molar site, measured 20 mm from the premolar site, and lastly the retromolar site, 15 mm posterior to the molar site. The distances were gauged with a periodontal probe (University of North Carolina [UNC] Probe, Hu-Friedy, Chicago, IL, USA) accurate to the nearest 1 mm. The ultrasound probe (L8-25, Zonare/Mindray, USA) was placed at each selected site to obtain a cross-sectional image in DICOM format. The built-in function in the ultrasound device for spatial compounding was selected to obtain well-resolved images (ZS3 Zonare/Mindray, USA). Acoustic coupling was achieved with the application of ultrasound gel (Aquasonic, Parker Inc., PA, USA) and the use of a gel-based stand-off-pad (Parker Inc.).

The captured ultrasound images were read with a commercially available software package (Osirix, Bernex, Switzerland) to obtain thickness measurements of the mucosal, mylohyoid, and the lingual nerve. At each site, the thickness of the mucosa and the mylohyoid muscle were measured at two distinct locations, 5- and 10-mm distances lingual to the muscle attachment to the mandible. In addition to the stated measurements, at the retromolar site, the lingual nerve diameter was also obtained. All measurements were carried out by a single calibrated examiner (SB) with a built-in device caliper accurate to 0.01 mm. The examiner calibration was performed, by measuring 10 random samples by the senior investigator (HC) and the assessment of accuracy and reproducibility in measurements by the chosen examiner (SB) to reach an agreement value of at least 0.86.

2.3. Biopsy sample collection and measurements

Immediately after the ultrasound images were captured from each cadaver head, a biopsy sample from the same imaged sites was collected by an operator with

expertise in cadaveric tissue handling and biopsy collection (SN) from the University of Michigan Anatomical Department of the Medical School. From each site, two samples, the mucosa and muscle tissues, were carefully collected. From the retromolar area a cross-sectional slice of the lingual nerve was also obtained (as imaged with the ultrasound). All collected samples were promptly placed in 10% formalin, and sent to the Histology Core at the University of Michigan Health System, Department of Pathology, Immunohistochemistry Laboratory, where they were imbedded in paraffin, and sectioned to three 5 micron-thick slices at every 5 mm interval from the attachment, as specifically marked at the harvesting procedure using a tissue coloring marker. Subsequently, all samples were stained with hematoxylin-eosin (H&E).

The specimens were viewed using an E800 Microscope (Nikon Instruments Inc., Melville, NY, USA) with a 2X objective to perform the measurements. Images were captured using a CoolSNAP EZ camera (Photometrics, Tucson, AZ, USA) and saved using a software (NIS-Elements Advanced, Nikon Corporation, Tokyo, Japan). To obtain the thickness measurements, each sample was measured at every third of the total sample length, and then averaged to obtain the measurement representative of that slide. This was performed for the collected samples of the mucosa and muscle. While for the nerve measurements, the diameter of each sample was measured twice in a way that the two measurements would be perpendicular to one another, and then averaged to obtain the cross-sectional (diameter) thickness of that nerve. All measurements were performed by a single calibrated examiner (SB). The software was able to conduct measurements with an accuracy 0.001 mm. The examiner calibration was performed prior to initiation of the measurement by randomly selecting 10 samples for measurement by the senior investigator (HC) and assessment of precision of the chosen examiner (SB) for reaching an agreement value of at least 0.86.

2.4. Clinical Feasibility of Imaging the Lingual Nerve

To assess the feasibility of imaging the lingual nerve with ultrasound, the second part of this study consisted of recruitment of healthy adult patients. The live human investigation part of the current study was approved by the Institutional Review Board for Human Studies (HUM00139630). The study was conducted at the Graduate Periodontal Clinic, Department of Periodontology and Oral Medicine, University of Michigan. It was conducted according to the principles embodied in the Helsinki Declaration of 1975, as revised in 2000 for biomedical research involving human subjects. The device setups and the scanning protocol followed the abovementioned methods. One experienced examiner (HC) performed the scanning of the lingual nerve; while the other examiner (OK) operated the scanning machine. Acquired ultrasound images were saved in DICOM files and interpreted with the same commercially available software (Osirix, Bernex, Switzerland). The lingual nerve dimension was measured with the built-in caliper accurate to 0.01 mm.

2.5. Data management and statistical analysis

All recorded measurements were entered into a spread sheet and checked for entry errors. For cadaverous data, descriptive statistics were used for qualitative presentation of the ultrasound and histology measurements by computation of means and standard deviations. To test the presence of statistically significance differences among the two modes of measurements, independent t-tests were utilized and a p-value threshold of 0.05 was set for significance. For live human data, the ultrasound lingual neve dimension was measured, presented as the mean and standard deviation. All analyses were conducted in Rstudio (Rstudio Version 1.1.383, RStudio, Inc., Massachusetts, USA) for Macintosh. Inter-examiner reliability calibration tests were performed with the DescTools package (Signorell, 2019).

3. Results

The lingual anatomical structures of 9 human cadaver heads were imaged using ultrasound. Biopsy samples corresponding to the imaged sites were also successfully collected from every site. The means and standard deviations of

obtained measurements from the ultrasound and histology were summarized in Table 1.

3.1. Imaging Interpretation

The mylohyoid is a hypoechoic (dark) band with relatively uniform thickness along its length (Figure 2 - left). Within it is hyperechoic (white) strips. It attaches to the mandible at one end and extends apically and lingually toward the tongue. Above it is the mucosal layer and the sublingual space, containing the sublingual gland; below it is the submandibular space. The lingual nerve has its characteristic hyperechoic continuous bundles of neuronal fascicles separated from surrounding hypoechoic connective tissue (Figure 2 - right). Anatomically, it lies above the mylohyoid muscle at the retromolar area. In this case, it is located superficially, just below the mucosal layer. Figure 3 depicted representative histologic images of the lingual mucosa, mylohyoid muscle and lingual nerve.

3.2. Dimension comparisons

The overall mean ultrasound mucosal thickness was 1.45 ± 0.49 mm at 5 mm distance to the muscle attachment (1.44 mm in the premolar, 1.31 in the molar, and 1.58 in the retromolar region), and 1.54 ± 0.48 mm at the 10 mm distance to the attachment (1.46 mm in the premolar, 1.35 in the molar, and 1.76 mm in the retromolar region). The corresponding histologic mucosal thickness at the respective sites averaged to 1.39 ± 0.51 mm at the 5 mm distance to the attachment (1.46 mm in the premolar, 1.30 in the molar, and 1.44 mm in the retromolar region), and 1.37 ± 0.46 mm at 10 mm distance to the attachment (1.28, 1.16, and 1.61 mm in the premolar, molar, retromolar region, respectively). The differences among the obtained values from the ultrasound compared to the biopsied samples did not reach statistical significance ($p>0.05$) when tested as a whole, and among each respective region.

In regard to the mylohyoid muscle thickness measurements, the overall ultrasound mean value was 2.31 ± 0.56 at 5 mm from the attachment (2.03 mm for the premolar area, 2.59 mm at the molar, and 2.22 mm at the retromolar region), and 2.46 ± 0.56 mm at 10 mm distance to the attachment (2.28 mm at

the premolar, 2.75 mm at the molar, and 2.33 mm at the retromolar area). The corresponding histologic values have an overall mean of 2.25 ± 0.47 mm at the 5 mm distance (2.04 mm for premolar, 2.46 for the molar, and 2.22 for the retromolar regions), and 2.36 ± 0.50 mm at the 10 mm distance to the attachment (2.23, 2.56, and 2.22 mm at the premolar, molar and retromolar regions, respectively). Again, there was no significant differences between ultrasound and histology in any of the obtained mylohyoid muscle thickness measurements ($p>0.05$ for all comparisons).

Lastly, as for the measurements of the lingual nerve diameter, similar values were obtained via ultrasound (2.38 ± 0.44 mm), and histological assessments (2.43 ± 0.42 mm) without statistically significant difference ($p>0.05$).

3.3. Outcomes of live human scans

A total of 19 individuals, corresponding to 30 sites (18 on the right, and 12 on the left) were available for ultrasound imaging of the lingual nerve in the retromolar area. The mean diameter was 2.11 ± 0.35 mm (ranging from 1.49 – 3.14 mm). The mean values between the right and left sides were not significantly different (2.02 ± 0.25 mm vs. 1.99 ± 0.47 mm, $p=0.79$). Figure 4 displays a cross-sectional image of a lingual nerve in a live human participant, and Figure 5 shows the distribution of the lingual nerve diameter.

5. Discussion

For the first time in the literature, ultrasound was found accurate in imaging the human mucosal, mylohyoid muscle and lingual nerve because of (1) dimensional consistency with histology and the literature and (2) imaging characters in accordance with other nerves and muscles. Our study concluded ultrasound and histologic dimensions of the abovementioned structures are not statistically different. A recent study (Kikuta, Iwanaga, Kusukawa, & Tubbs, 2019) showed the mean diameter of the lingual nerve is 2.2 mm (range 1.61 – 2.95 mm), which is in agreement with our measurements on human cadavers as well

as live humans. The sheath-like hyperechoic appearance of the lingual nerve on ultrasound images is consistent with nerve fascicles. The hypoechoic band representing mylohyoid muscle is also characteristic of muscles in the rest of the body (Engel, Harn, & Cohen, 1987; Koolstra & van Eijden, 1999).

Anatomy of the mandibular lingual region has becoming more important than ever because of the popularity of performing ridge augmentation for implant placement in this region. Lingual flap releasing for achieving primary wound closure requires detachment of the lingual mucosa from the underlying mylohyoid muscle. Knowledge about the lingual mucosa thickness, sublingual salivary glands, and mylohyoid muscle attachment is key to successful lingual flap management. This study showed that the mean mucosal thickness is approximately 1.5 mm. Histology also showed that the submucosa is mainly composed of adipose tissue. The thin dimension and loose tissue consistency reaffirmed difficulties in managing the lingual flap clinically. The mean mylohyoid muscle dimension is approximately 2.5 mm. What may be more important is the location of the muscle attachment because it determines the degree of difficulty in releasing the lingual flap. When the attachment is high, i.e. closer to the alveolar crest, flap releasing is more challenge and vice versa. Knowledge about the mylohyoid muscle location and lingual mucosa features pre-surgery could be beneficial to assess the risk of wound opening after ridge augmentation.

The lingual nerve is a branch of the mandibular nerve, providing sensory innervation to the mucous membranes of the anterior two-thirds of the tongue and the lingual tissues. After entering the oral cavity, it is located at a mean distance of 3 mm apical to the osseous crest and 2 mm horizontally from the lingual cortical plate in the third molar area. (Behnia, Kheradvar, & Shahrokhi, 2000). Nevertheless, the nerve may be situated at or above the crest of bone in 15 to 20% cases (Pogrel & Goldman, 2004). Furthermore, 22% of the time the nerve may contact the lingual cortical plate.(Behnia et al., 2000). Once passing the 3rd molar, it travels mesially, apically, and medially towards the tongue. The vertical distance between the nerve and the cementoenamel junction (CEJ) of the second molar, first molar and the second premolar was 9.6, 13 and 14.8 mm,

respectively (Chan et al., 2011). Because its superficial location in the 3rd molar region, precaution has to be exercised when performing a flap surgery in this area. A 0.6% to 2% incidence of lingual nerve injury has been reported following third molar extraction.(Bataineh, 2001; Gomes, Vasconcelos, de Oliveira e Silva, & da Silva, 2005; Gulicher & Gerlach, 2001; Hillerup & Stoltze, 2007; Valmaseda-Castellon, Berini-Aytes, & Gay-Escoda, 2000). Ultrasound is an optimal imaging modality for this neve because it cannot be seen on radiographs. Our group published a proof-of-principle study showing ultrasound can image the intact lingual nerve. (19) The present study with a larger sample size and application in live humans, further confirmed the accuracy of ultrasound in imaging this nerve. Earlier reports of investigating the lingual nerve, while with a different methodology, can also been noted in the literature. Olson et al. using a slightly larger ultrasound device (25 mm transducer, 10-5 MHz) analyzed the lingual nerve in 9 pig cadaveric specimens, in an attempt to correctly identify an intact, partially transected, or fully transected injury to the nerve (Olsen et al., 2007). Later on, Al-Amery and colleagues, using ultrasound on previously dissected, and harvested lingual nerves from 6 human cadavers were able to visualize the bur-induced lacerations at the damaged sites (Al-Amery, Ngeow, Nambiar, & Naidu, 2018).

Another clinical indication for locating the lingual nerve is for its block anesthesia. The most common target for local anesthesia of the lingual nerve is the pterygomandibular space. However, inadequate anesthesia of the lingual nerve is common because of unreliable landmarks (Balasubramanian et al., 2017). Exclusive lingual nerve block at the 3rd molar region could be an effective alternative because of the following advantages: (1) easier and closer access, (2) aspiration is not required because of no major vessels in this area, and (3) less chance of post-injection trismus. Visualization of the nerve with ultrasound may improve clinician confidence, increase anesthesia success rate and working time, and reduce injection quantity. Moreover, ultrasound could be a learning tool for dental students to practice lingual nerve anesthesia.

6. Conclusion

This study successfully characterizes important anatomical structures in the lingual mandible, including the mucosa, the mylohyoid muscle, and the lingual nerve with non-invasive, non-radiation and chairside ultrasound. This novel imaging modality may become a useful tool to evaluate lingual anatomy and assess the risk of developing complications, particularly prior to a surgery.

Conflict of interest:

The authors do not have any financial interests, either directly or indirectly, in the products or information listed in the paper. The study was supported by grants from the Delta Dental Foundation (PAF01878), the Osteology Foundation (PAF06301), Department of Periodontics and Oral Medicine Clinical Research Supplemental Research Grant, School of Dentistry Research Collaborative Award (U054647) and a NIDCR grant (1R21DE027765).

Acknowledgments:

The authors would like to thank the body donors and their families, Mr. Dean Mueller, Coordinator of the Anatomical Donations Program for preparing the specimens, Mrs. Alicia Baker, Clinical Coordinator, and Ms. Cynthia Miller, Dental Assistant, for kindly coordinating the experiment. We also give thanks to Kenneth Rieger, Multimedia Designer, the University of Michigan for his effort in the drawing of the illustration.

Author contributions:

SB contributed to conception and design, drafted and critically revised the manuscript, performed the ultrasound and histology measurements and analyzed the data; HLC, contributed to conception and design, mentored the project, performed the ultrasound scans, drafted and critically revised the manuscript; SN, performed the biopsy specimens, drafted and critically revised the manuscript; HLW, contributed to conception, design, and critically revised the manuscript, OK, contributed to conception and design, performed the ultrasound

scans, drafted and critically revised the manuscript. All authors gave final approval and agree to be accountable for all aspects of the work.

REFERENCES

Al-Amery, S. M., Ngeow, W. C., Nambiar, P., & Naidu, M. (2018). A pilot study on the effects of direct contact of two different surgical burs on the cadaveric lingual nerve. *Int J Oral Maxillofac Surg, 47*(9), 1153-1160. doi:10.1016/j.ijom.2018.04.013

Annibali, S., Ripari, M., La Monaca, G., Tonoli, F., & Cristalli, M. P. (2009). Local accidents in dental implant surgery: prevention and treatment. *Int J Periodontics Restorative Dent, 29*(3), 325-331.

Askar, H., Di Gianfilippo, R., Ravida, A., Tattan, M., Majzoub, J., & Wang, H. L. (2019). Incidence and severity of postoperative complications following oral, periodontal, and implant surgeries: A retrospective study. *J Periodontol*. doi:10.1002/JPER.18-0658

Balasubramanian, S., Paneerselvam, E., Guruprasad, T., Pathumai, M., Abraham, S., & Krishnakumar Raja, V. B. (2017). Efficacy of Exclusive Lingual Nerve Block versus Conventional Inferior Alveolar Nerve Block in Achieving Lingual Soft-tissue Anesthesia. *Ann Maxillofac Surg, 7*(2), 250-255. doi:10.4103/ams.ams_65_17

Bataineh, A. B. (2001). Sensory nerve impairment following mandibular third molar surgery. *J Oral Maxillofac Surg, 59*(9), 1012-1017; discussion 1017. doi:S0278-2391(01)58639-5 [pii]

10.1053/joms.2001.25827

Behnia, H., Kheradvar, A., & Shahrokhi, M. (2000). An anatomic study of the lingual nerve in the third molar region. *Journal of oral and maxillofacial surgery, 58*(6), 649-651; discussion 652.

Bhaskar, V., Chan, H. L., MacEachern, M., & Kripfgans, O. D. (2018). Updates on ultrasound research in implant dentistry: a systematic review of potential clinical indications. *Dentomaxillofac Radiol, 47*(6), 20180076. doi:10.1259/dmfr.20180076

Camargo, I. B., & Van Sickels, J. E. (2015). Surgical complications after implant placement. *Dent Clin North Am, 59*(1), 57-72. doi:10.1016/j.cden.2014.08.003

Chan, H. L., Benavides, E., Yeh, C. Y., Fu, J. H., Rudek, I. E., & Wang, H. L. (2011). Risk assessment of lingual plate perforation in posterior mandibular region: a virtual implant placement study using cone-beam computed tomography. *J Periodontol, 82*(1), 129-135. doi:10.1902/jop.2010.100313

Chan, H. L., Leong, D. J., Fu, J. H., Yeh, C. Y., Tatarakis, N., & Wang, H. L. (2010). The significance of the lingual nerve during periodontal/implant surgery. *J Periodontol, 81*(3), 372-377. doi:10.1902/jop.2009.090506

Chan, H. L., Sinjab, K., Chung, M. P., Chiang, Y. C., Wang, H. L., Giannobile, W. V., & Kripfgans, O. D. (2017). Non-invasive evaluation of facial crestal bone with ultrasonography. *PLoS One, 12*(2), e0171237. doi:10.1371/journal.pone.0171237

Chan, H. L., Sinjab, K., Li, J., Chen, Z., Wang, H. L., & Kripfgans, O. D. (2018). Ultrasonography for noninvasive and real-time evaluation of peri-implant tissue dimensions. *J Clin Periodontol, 45*(8), 986-995. doi:10.1111/jcpe.12918

Chan, H. L., Wang, H. L., Fowlkes, J. B., Giannobile, W. V., & Kripfgans, O. D. (2017). Non-ionizing real-time ultrasonography in implant and oral surgery: A feasibility study. *Clin Oral Implants Res, 28*(3), 341-347. doi:10.1111/clr.12805

Chao, Y. C., Chang, P. C., Fu, J. H., Wang, H. L., & Chan, H. L. (2015). Surgical Site Assessment for Soft Tissue Management in Ridge Augmentation Procedures. *Int J Periodontics Restorative Dent, 35*(5), e75-83. doi:10.11607/prd.2097

Chen, S. H., Chan, H. L., Lu, Y., Ong, S. H., Wang, H. L., Ko, E. H., & Chang, P. C. (2017). A Semi-automatic Algorithm for Preliminary Assessment of Labial Gingiva and Alveolar Bone Thickness of Maxillary Anterior Teeth. *Int J Oral Maxillofac Implants, 32*(6), 1273-1280. doi:10.11607/jomi.5566

De Bruyckere, T., Eghbali, A., Younes, F., De Bruyn, H., & Cosyn, J. (2015). Horizontal stability of connective tissue grafts at the buccal aspect of single implants: a 1-year prospective case series. *J Clin Periodontol, 42*(9), 876-882. doi:10.1111/jcpe.12448

De Rouck, T., Eghbali, R., Collys, K., De Bruyn, H., & Cosyn, J. (2009). The gingival biotype revisited: transparency of the periodontal probe through the gingival margin as a method to discriminate thin from thick gingiva. *J Clin Periodontol, 36*(5), 428-433. doi:10.1111/j.1600-051X.2009.01398.x

Eghbali, A., De Rouck, T., De Bruyn, H., & Cosyn, J. (2009). The gingival biotype assessed by experienced and inexperienced clinicians. *J Clin Periodontol, 36*(11), 958-963. doi:10.1111/j.1600-051X.2009.01479.x

Engel, J. D., Harn, S. D., & Cohen, D. M. (1987). Mylohyoid herniation: gross and histologic evaluation with clinical correlation. *Oral Surg Oral Med Oral Pathol, 63*(1), 55-59. doi:10.1016/0030-4220(87)90340-9

Ferrus, J., Cecchinato, D., Pjetursson, E. B., Lang, N. P., Sanz, M., & Lindhe, J. (2010). Factors influencing ridge alterations following immediate implant placement into extraction sockets. *Clin Oral Implants Res, 21*(1), 22-29. doi:10.1111/j.1600-0501.2009.01825.x

Fu, J. H., Yeh, C. Y., Chan, H. L., Tatarakis, N., Leong, D. J., & Wang, H. L. (2010). Tissue biotype and its relation to the underlying bone morphology. *J Periodontol, 81*(4), 569-574. doi:10.1902/jop.2009.090591

Gomes, A. C., Vasconcelos, B. C., de Oliveira e Silva, E. D., & da Silva, L. C. (2005). Lingual nerve damage after mandibular third molar surgery: a randomized clinical trial. *J Oral Maxillofac Surg, 63*(10), 1443-1446. doi:S0278-2391(05)01033-5 [pii]
10.1016/j.joms.2005.06.012

Greenstein, G., Cavallaro, J., Romanos, G., & Tarnow, D. (2008). Clinical recommendations for avoiding and managing surgical complications associated with implant dentistry: a review. *J Periodontol, 79*(8), 1317-1329. doi:10.1902/jop.2008.070067

Gulicher, D., & Gerlach, K. L. (2001). Sensory impairment of the lingual and inferior alveolar nerves following removal of impacted mandibular third molars. *Int J Oral Maxillofac Surg, 30*(4), 306-312. doi:S0901-5027(01)90057-8 [pii]
10.1054/ijom.2001.0057

Hillerup, S., & Stoltze, K. (2007). Lingual nerve injury in third molar surgery I. Observations on recovery of sensation with spontaneous healing. *Int J Oral Maxillofac Surg, 36*(10), 884-889. doi:S0901-5027(07)00231-7 [pii]
10.1016/j.ijom.2007.06.004

Hoskins, P. R., & Kenwright, D. A. (2015). Recent developments in vascular ultrasound technology. *Ultrasound, 23*(3), 158-165. doi:10.1177/1742271X15578778

Isaacson, T. J. (2004). Sublingual hematoma formation during immediate placement of mandibular endosseous implants. *J Am Dent Assoc, 135*(2), 168-172. doi:10.14219/jada.archive.2004.0148

Kikuta, S., Iwanaga, J., Kusukawa, J., & Tubbs, R. S. (2019). An anatomical study of the lingual nerve in the lower third molar area. *Anat Cell Biol, 52*(2), 140-142. doi:10.5115/acb.2019.52.2.140

Koolstra, J. H., & van Eijden, T. M. (1999). Three-dimensional dynamical capabilities of the human masticatory muscles. *J Biomech, 32*(2), 145-152.

Lin, G. H., Chan, H. L., & Wang, H. L. (2013). The significance of keratinized mucosa on implant health: a systematic review. *J Periodontol, 84*(12), 1755-1767. doi:10.1902/jop.2013.120688

Linkevicius, T., Apse, P., Grybauskas, S., & Puisys, A. (2009a). The influence of soft tissue thickness on crestal bone changes around implants: a 1-year prospective controlled clinical trial. *Int J Oral Maxillofac Implants, 24*(4), 712-719.

Linkevicius, T., Apse, P., Grybauskas, S., & Puisys, A. (2009b). Reaction of crestal bone around implants depending on mucosal tissue thickness. A 1-year prospective clinical study. *Stomatologija, 11*(3), 83-91.

Longoni, S., Sartori, M., Braun, M., Bravetti, P., Lapi, A., Baldoni, M., & Tredici, G. (2007). Lingual vascular canals of the mandible: the risk of bleeding complications during implant procedures. *Implant Dent, 16*(2), 131-138. doi:10.1097/ID.0b013e31805009d5

Moskalik, A., Carson, P. L., Meyer, C. R., Fowlkes, J. B., Rubin, J. M., & Roubidoux, M. A. (1995). Registration of three-dimensional compound ultrasound scans of the breast for refraction and motion correction. *Ultrasound Med Biol, 21*(6), 769-778.

O'Brien, B. C., Harris, I. B., Beckman, T. J., Reed, D. A., & Cook, D. A. (2014). Standards for reporting qualitative research: a synthesis of recommendations. *Acad Med, 89*(9), 1245-1251. doi:10.1097/ACM.0000000000000388

Oelze, M. L., & Mamou, J. (2016). Review of Quantitative Ultrasound: Envelope Statistics and Backscatter Coefficient Imaging and Contributions to Diagnostic Ultrasound. *IEEE Trans Ultrason Ferroelectr Freq Control, 63*(2), 336-351. doi:10.1109/TUFFC.2015.2513958

Olsen, J., Papadaki, M., Troulis, M., Kaban, L. B., O'Neill, M. J., & Donoff, B. (2007). Using ultrasound to visualize the lingual nerve. *J Oral Maxillofac Surg, 65*(11), 2295-2300. doi:10.1016/j.joms.2007.06.647

Pogrel, M. A., & Goldman, K. (2004). Lingual flap retraction for third molar removal. *Journal of oral and maxillofacial surgery, 62*(9), 1125-1130.

Ritter, L., Neugebauer, J., Mischkowski, R. A., Dreiseidler, T., Rothamel, D., Richter, U., . . . Zoller, J. E. (2012). Evaluation of the course of the inferior alveolar nerve in the mental foramen by cone beam computed tomography. *Int J Oral Maxillofac Implants, 27*(5), 1014-1021.

Signorell, A. (2019). DescTools: Tools for Descriptive Statistics.

Suarez-Lopez Del Amo, F., Lin, G. H., Monje, A., Galindo-Moreno, P., & Wang, H. L. (2016). Influence of Soft Tissue Thickness on Peri-Implant Marginal Bone Loss: A Systematic Review and Meta-Analysis. *J Periodontol, 87*(6), 690-699. doi:10.1902/jop.2016.150571

Tavelli, L., Barootchi, S., Namazi, S. S., Chan, H. L., Brzezinski, D., Danciu, T., & Wang, H. L. (2019). The influence of palatal harvesting technique on the donor site vascular injury: A split-mouth comparative cadaver study. *J Periodontol*. doi:10.1002/JPER.19-0073

Tavelli, L., Barootchi, S., Ravida, A., Oh, T. J., & Wang, H. L. (2019). What Is the Safety Zone for Palatal Soft Tissue Graft Harvesting Based on the Locations of the Greater Palatine Artery and Foramen? A Systematic Review. *J Oral Maxillofac Surg, 77*(2), 271 e271-271 e279. doi:10.1016/j.joms.2018.10.002

Urban, I., Traxler, H., Romero-Bustillos, M., Farkasdi, S., Bartee, B., Baksa, G., & Avila-Ortiz, G. (2018). Effectiveness of Two Different Lingual Flap Advancing

Techniques for Vertical Bone Augmentation in the Posterior Mandible: A Comparative, Split-Mouth Cadaver Study. *Int J Periodontics Restorative Dent, 38*(1), 35-40. doi:10.11607/prd.3227

Urban, I. A., Monje, A., Wang, H. L., Lozada, J., Gerber, G., & Baksa, G. (2017). Mandibular Regional Anatomical Landmarks and Clinical Implications for Ridge Augmentation. *Int J Periodontics Restorative Dent, 37*(3), 347-353. doi:10.11607/prd.3199

Valmaseda-Castellon, E., Berini-Aytes, L., & Gay-Escoda, C. (2000). Lingual nerve damage after third lower molar surgical extraction. *Oral Surg Oral Med Oral Pathol Oral Radiol Endod, 90*(5), 567-573. doi:S1079-2104(00)56151-4 [pii] 10.1067/moe.2000.110034

Table 1. Ultrasound and histologic measurements of the anatomical structures of the lingual mandible.

	5 mm	**10 mm**

Structure	Site	Ultrasound	Histology	*p* value	Ultrasound	Histology	*p* value
Mucosa	Premolar	1.448 ± 0.402	1.460 ± 0.441	0.957	1.467 ± 0.505	1.280 ± 0.501	0.469
	Molar	1.317 ± 0.536	1.301 ± 0.58	0.959	1.358 ± 0.391	1.168 ± 0.391	0.391
	Retromolar	1.581 ± 0.531	1.440 ± 0.512	0.531	1.761 ± 0.512	1.619 ± 0.512	0.521
	Overall	1.453 ± 0.496	1.398 ± 0.507		1.541 ± 0.489	1.370 ± 0.496	
Muscle	Premolar	2.037 ± 0.449	2.044 ± 0.441	0.976	2.282 ± 0.631	2.231 ± 0.579	0.862
	Molar	2.590 ± 0.646	2.461 ± 0.466	0.598	2.751 ± 0.538	2.567 ± 0.472	0.414
	Retromolar	2.227 ± 0.471	2.225 ± 0.475	0.827	2.334 ± 0.471	2.227 ± 0.455	0.781
	Overall	2.316 ± 0.564	2.256 ± 0.478		2.467 ± 0.568	2.367 ± 0.505	
Nerve	Retromolar	2.386 ± 0.441	2.432 ± 0.423	0.785			

All reported values are in mm ± standard deviation

p values are from independent t-tests

Figure Legends:

Figure 1. Schematic illustration of the measurements performed on ultrasound and histology on the fresh human cadaveric specimens.

Figure 2. Ultrasound images of (A) the mylohyoid muscle and adjacent structures and (B) the lingual nerve. M: mucosa; SLG: sublingual gland; Att:

mylohyoid muscle attachment; MM: mylohyoid muscle; LP: lingual plate of the mandible; N: lingual nerve.

Figure 3. Histology images of the lingual nerve (A), mucosa (B), and the mylohyoid muscle (C).

Figure 4. An obtained ultrasound image of the lingual nerve in a live human subject.

Figure 5. Scatter plot displaying the distribution of the lingual nerve diameters in live patients.

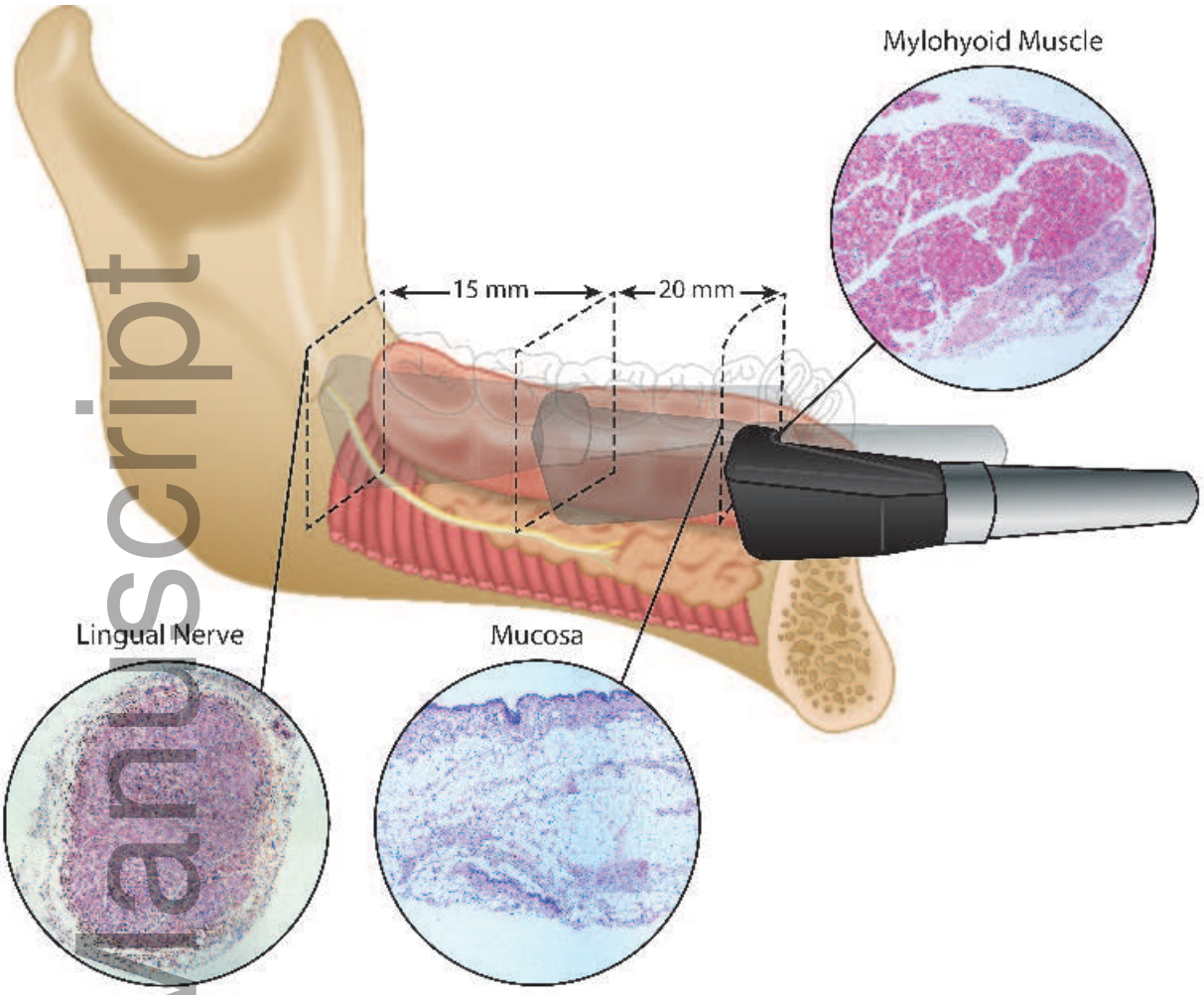

clr_13573_f1.tif

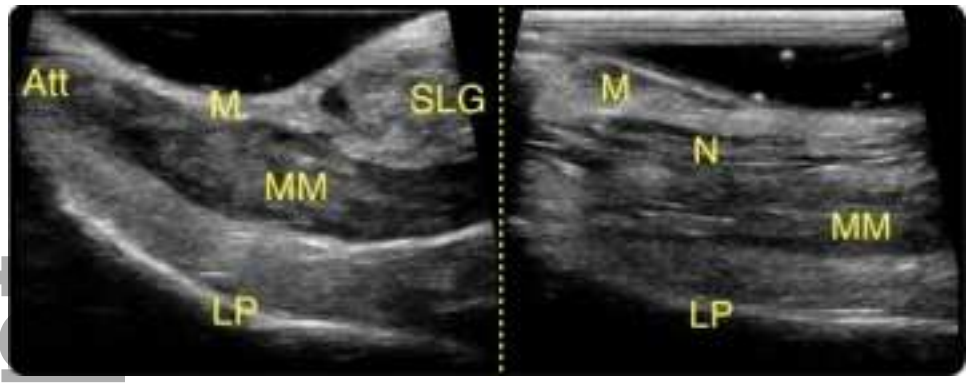

clr_13573_f2.tiff

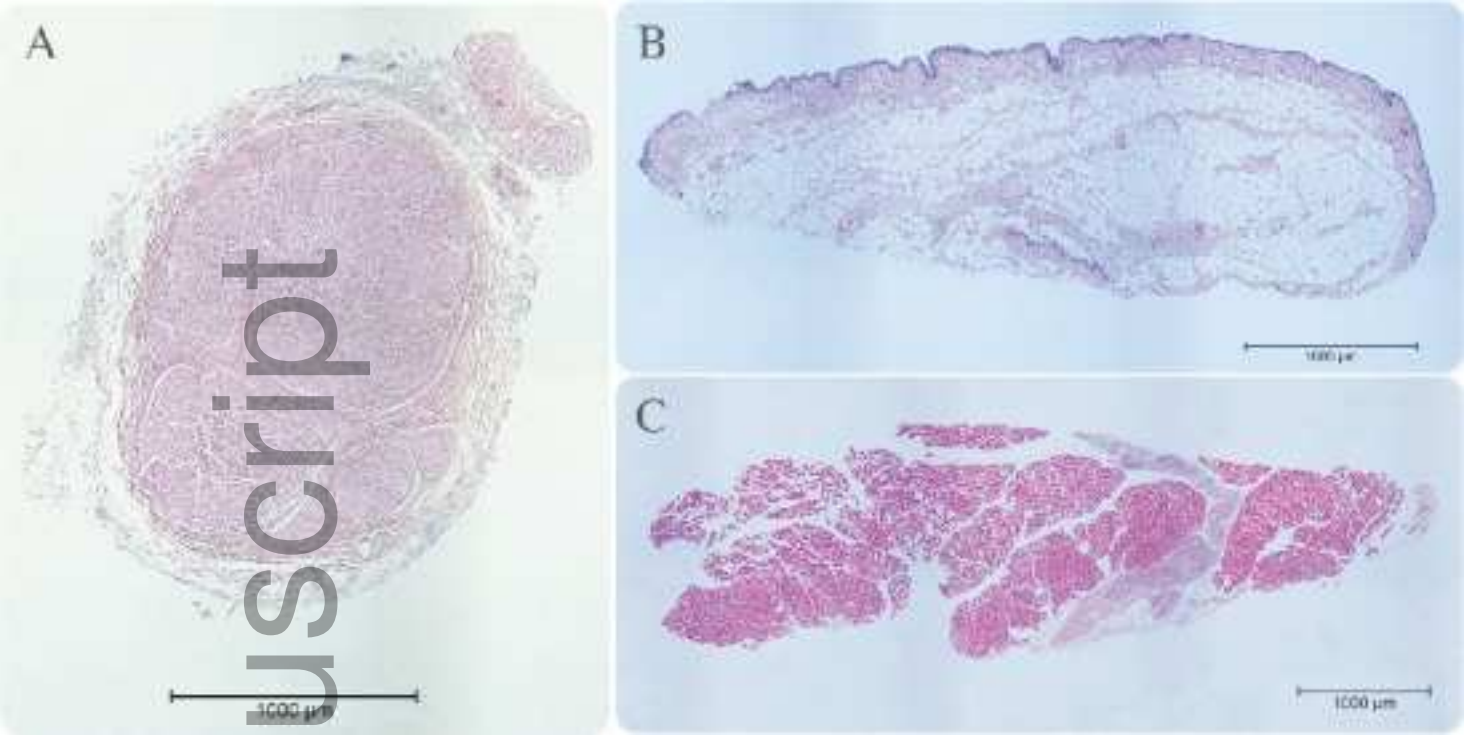

clr_13573_f3.tif

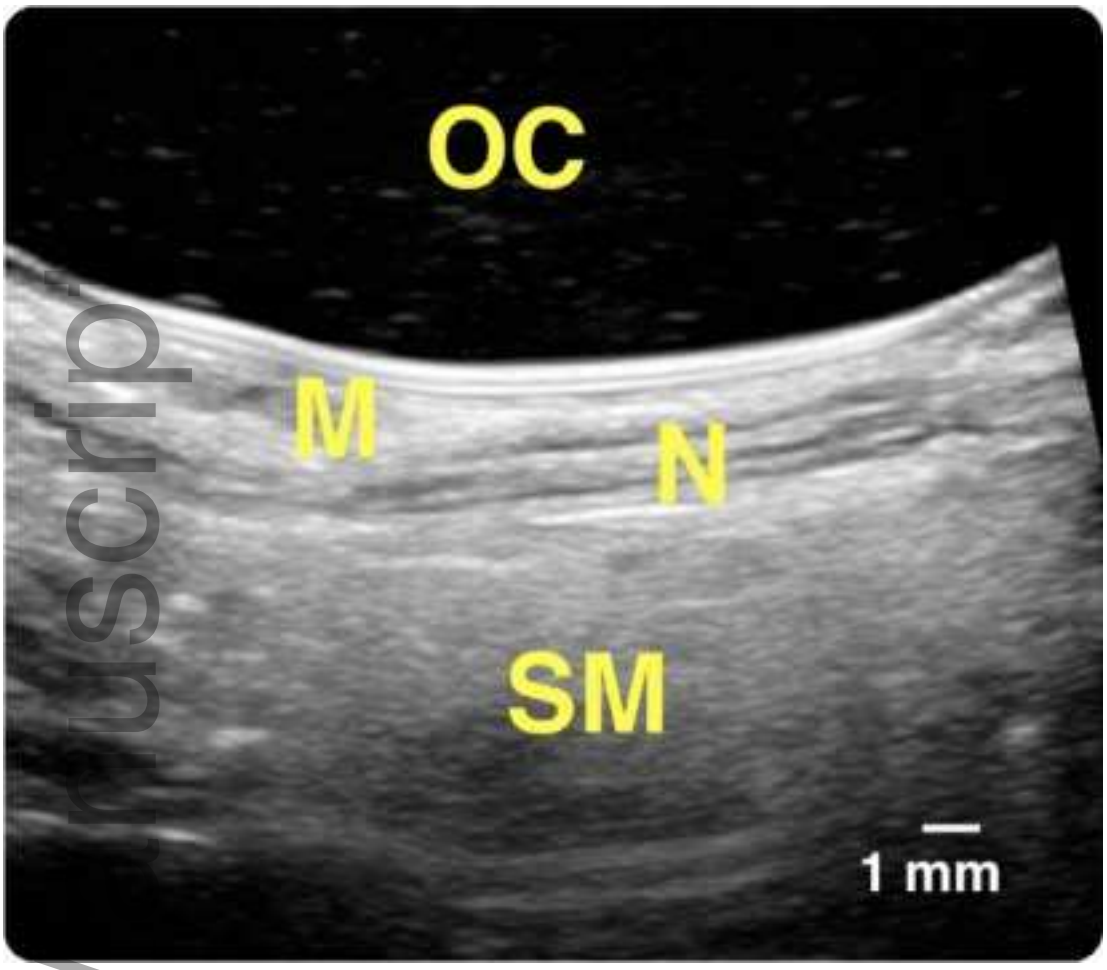

clr_13573_f4.tiff

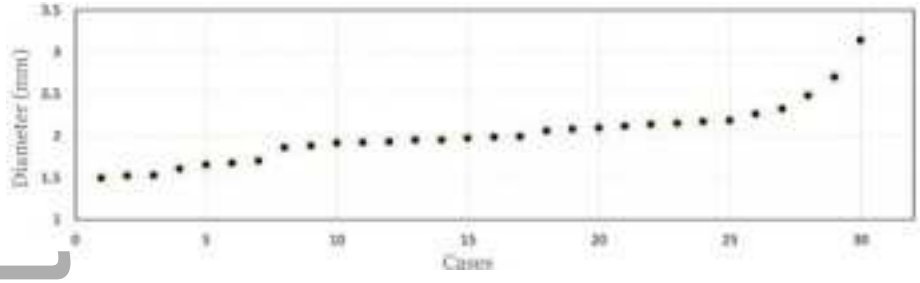

clr_13573_f5.tif